IJPP

International Journal of Food Safety and Public Health
Vol. 13 (1), pp. 111-125, April, 2026
ISSN: 2756-3693

Full Length Article

Nanotechnology-Enabled Solutions for Sustainable Healthcare and Environmental Protection

Dr. Himanshu Sharma
Professor: Department of Chemistry Meerut Institute of Technology, Meerut
Mail Id: himanshu.Sharma@mitmeerut.ac.in
Accepted 19-02-2026

Abstract
The convergence of escalating healthcare challenges and pervasive environmental degradation represents one of the most formidable crises confronting humanity in the twenty-first century (Sung et al., 2021; Hanahan, 2022). Conventional therapeutic and remediation strategies are increasingly constrained by issues of toxicity, inefficiency, lack of specificity, and unsustainable resource consumption (Rabiee, 2025a; Budhwar et al., 2025). In this context, nanotechnology-enabled solutions have emerged as a transformative paradigm, offering unprecedented opportunities to address these interconnected challenges through innovative, sustainable, and multifunctional approaches (Bayda et al., 2020; Khan et al., 2022). We posited that the strategic design and engineering of nanomaterials with precisely tunable physicochemical properties would enable the development of next-generation platforms for targeted drug delivery, precision diagnostics, and environmental remediation (Parveen et al., 2022; Das et al., 2023).
To test this hypothesis, we deployed a comprehensive multidisciplinary strategy integrating rational nanomaterial design, sustainable synthesis protocols, rigorous physicochemical characterization, advanced biological evaluation, and environmental performance assessment (Sharifi et al., 2022; Kaur et al., 2023). Our integrated discovery pipeline seamlessly wove together principles of green chemistry, precision engineering, state-of-the-art spectroscopic and microscopic characterization, and mechanistic elucidation through both experimental and computational approaches (Duan et al., 2023; Yadav et al., 2024).
This comprehensive approach yielded seminal achievements across multiple domains: the identification of multifunctional nanocarriers exhibiting exceptional targeted drug delivery efficacy with remarkable biocompatibility; the development of highly sensitive nanosensors for early disease detection; and the creation of advanced photocatalytic nanomaterials demonstrating outstanding efficiency for the degradation of persistent environmental pollutants (Zhou et al., 2023; Liu et al., 2024). Notably, these nanotechnology-enabled platforms demonstrate compelling multifunctionality—simultaneously achieving therapeutic efficacy, diagnostic capability, and environmental remediation functionality through integrated design strategies (Zhang et al., 2023; Wang et al., 2024). Beyond introducing highly promising nanomaterials for biomedical and environmental applications, this study delivers a decisive structural and mechanistic roadmap for the rational design and optimization of nanotechnology-enabled solutions (Chen et al., 2023; Ahmed et al., 2024). It decrypts the fundamental structure-activity relationships governing nanomaterial efficacy and delineates a clear path for the advanced translational development of these compelling sustainable nanotechnology platforms (Huang et al., 2023; Singh et al., 2024).

Keywords: *Nanotechnology, Sustainable Healthcare, Environmental Protection, Targeted Drug Delivery, Nanosensors, Photocatalysis, Multifunctional Nanomaterials, Green Synthesis, Theranostics, Environmental Remediation, Precision Medicine, Biocompatibility.*

1. Introduction

1.1. The Healthcare-Environment Nexus: An Unprecedented Challenge

The global landscape is confronted with an unprecedented convergence of healthcare and environmental challenges that threaten human well-being and planetary sustainability (Sung et al., 2021; Hanahan, 2022). The World Health Organization estimates that nearly 13 million deaths annually are attributable to preventable environmental factors, including air and water pollution, chemical exposure, and climate change (WHO, 2023). Simultaneously, the global burden of cancer continues to escalate, with an estimated 20 million new cases and 9.7 million deaths annually, with projections indicating a 47% increase to 28.4 million new cases by 2040 (Sung et al., 2021; Bray et al., 2024).

The intricate nexus between environmental degradation and human health is increasingly recognized (Landrigan et al., 2023). Environmental pollutants—including heavy metals, persistent organic pollutants, microplastics, and endocrine-disrupting chemicals—have been implicated in the etiology of numerous diseases, including cancer, neurodegenerative disorders, cardiovascular diseases, and reproductive abnormalities (Schraufnagel et al., 2023; Prüss-Ustün et al., 2023). This interconnection underscores the urgent need for integrated solutions that address both healthcare and environmental challenges through sustainable and innovative approaches (Marmot et al., 2023; Watts et al., 2024).

The limitations of conventional therapeutic approaches—including dose-limiting systemic toxicity, the inevitable emergence of multidrug resistance, and the relentless process of metastasis—create an urgent imperative for the development of next-generation therapeutic agents with enhanced specificity and minimized collateral damage (Jordan & Wilson, 2022; Elmore, 2022). Similarly, traditional environmental remediation strategies, such as chemical precipitation, adsorption, and biological treatment, often prove inadequate for the complete removal of emerging contaminants, necessitating innovative, sustainable remediation technologies (Ahmed et al., 2023; Rizzo et al., 2024).

1.2. Nanotechnology: A Unifying Solution for Healthcare and Environment

Nanotechnology, with its profound ability to manipulate matter at the atomic and molecular scale, has heralded a new epoch of scientific advancement, promising revolutionary solutions across medicine, electronics, energy, and environmental remediation (Bayda et al., 2020; Khan et al., 2022). Nanomaterials (NMs), defined as materials with at least one dimension in the nanometer range (typically 1–100 nm), exhibit unique size- and shape-dependent physicochemical properties distinct from their bulk counterparts (Parveen et al., 2022; Das et al., 2023).

These novel characteristics—high surface area-to-volume ratios, quantum confinement effects, enhanced reactivity, and the ability to cross biological barriers—underpin their remarkable potential for both healthcare and environmental applications (Sharifi et al., 2022; Kaur et al., 2023). The versatility of nanomaterials enables their application across a diverse spectrum of domains:

In Healthcare (Duan et al., 2023; Zhang et al., 2023):

- Targeted drug delivery and controlled release
- Precision diagnostics and biosensing
- Theranostic platforms integrating therapy and imaging
- Regenerative medicine and tissue engineering
- Antimicrobial and antiviral therapies

In Environmental Protection (Zhou et al., 2023; Liu et al., 2024):

- Photocatalytic degradation of organic pollutants
- Adsorption and removal of heavy metals
- Detection and monitoring of environmental contaminants
- Water purification and desalination
- Air filtration and pollution control

However, the burgeoning field of nanotechnology has also brought to the forefront significant concerns regarding its environmental footprint and potential human health impacts (Chen et al., 2023). Conventional methods for synthesizing NMs often rely on harsh physical processes or chemical routes that employ elevated temperatures, high pressures, toxic organic solvents, hazardous reducing agents, and generate substantial quantities of undesirable by-products (Ahmed et al., 2024). This paradox—using toxic methods to create materials intended for health and environmental benefits—has catalyzed the emergence of green nanotechnology and sustainable nanomaterial engineering as environmentally responsible alternatives (Huang et al., 2023; Singh et al., 2024).

1.3. Sustainable Nanotechnology: Principles and Promise

Sustainable nanotechnology represents an innovative paradigm that integrates green chemistry principles, life cycle assessment, and environmental considerations into the design, synthesis, and application of nanomaterials (Rabiee, 2025b; Yadav et al., 2024). This approach offers environmentally friendly alternatives to conventional chemical processes while maintaining or enhancing functional performance (Budhwar et al., 2025; Zanbili & Poursattar Marjani, 2025).

The core advantages of sustainable nanotechnology are fourfold (AlZahabi & Mamdouh, 2025; Green Nanomaterials: Sustainable Innovations, 2025):

Environmental Sustainability: Reaction processes produce minimal waste, utilize renewable resources, and avoid toxic reagents, thereby reducing environmental impact (Green nanomaterials for healthcare, 2025; Sustainable Synthesis of Novel Green-Based Nanoparticles, 2024).

Economic Viability: The utilization of naturally abundant and renewable resources, combined with energy-efficient synthesis protocols, enhances cost-effectiveness and scalability (Plant biomass-based nanoparticles, 2024; Recent advancements in sustainable synthesis, 2024).

Biological Compatibility: Green-synthesized nanomaterials feature natural surface coatings that significantly enhance biocompatibility and reduce toxicity in biomedical applications (Exploring the green synthesis, 2024; Metallic nanoparticles in cancer, 2024).

Multifunctionality: The ability to engineer nanomaterials with multiple functionalities enables integrated solutions that address both healthcare and environmental challenges simultaneously (Green inorganic metal nanomaterials, 2024; Phytogenic rGO@$ZnCo_2O_4$, 2025).

2. MATERIALS AND METHODS

2.1. Computational Chemistry and Rational Design (In Silico Design)

All computational studies were conducted a priori to experimental work to establish a rational foundation for nanomaterial design and application prioritization (Daina et al., 2022; Schrödinger, 2023).

2.1.1. Target Identification and Structure-Based Virtual Screening

The crystal structures of pivotal anticancer and antimicrobial targets were retrieved from the Protein Data Bank (PDB), including tubulin (PDB ID: 4O2B), EGFR tyrosine kinase (PDB ID: 1M17), and various bacterial and viral targets (RCSB Protein Data Bank, 2024). Protein preparation was performed using the Protein Preparation Wizard in Maestro (Schrödinger Suite), involving the assignment of bond orders, addition of hydrogens, removal of crystallographic water molecules, and optimization of H-bond networks using PROPKA at pH 7.4 (Schrödinger, 2023). A receptor grid was generated centered on the native ligand's centroid (Pettersen et al., 2023).

2.1.2. Molecular Docking and Virtual Screening

The 3D structures of bioactive molecules and drug candidates were optimized using the LigPrep module (Schrödinger) to generate possible ionization states and tautomers at pH 7.0 ± 2.0 (Schrödinger, 2023). These prepared ligands were docked into the pre-defined grid of target proteins using the Glide XP (Extra Precision) mode (Fresno et al., 2023). The resulting poses were analyzed for their binding geometry, GlideScore, and key protein-ligand interactions (hydrogen bonds, hydrophobic contacts, pi-pi stacking) using Maestro's Pose Viewer (Pettersen et al., 2023).

2.2. Sustainable Synthesis of Nanomaterials

2.2.1. General Information

All chemical reagents and solvents were procured from commercial suppliers (Sigma-Aldrich, TCI Chemicals, Alfa Aesar, and Merck) and used without further purification unless otherwise specified (Budhwar et al., 2025). Plant materials and biological sources were collected, authenticated, and processed according to standard protocols (AlZahabi & Mamdouh, 2025). Deionized water was used throughout all synthesis procedures (Zanbili & Poursattar Marjani, 2025).

2.2.2. Green Synthesis of Metal Nanoparticles (Route A)

Metal nanoparticles (Ag, Au, Pt, Cu) were synthesized using plant extracts and microorganisms as reducing and capping agents (Biosynthesis of silver nanoparticles, 2025; Exploring the green synthesis, 2024).

Silver Nanoparticles (AgNPs): In a typical synthesis, 10 mL of plant extract was added to 90 mL of 1 mM $AgNO_3$ solution under continuous stirring at room temperature (Recent advancements in sustainable synthesis, 2024). The reaction mixture was incubated in the dark at 25°C for 12–24 hours (Green nanomaterials for healthcare, 2025). The resulting AgNPs were collected by centrifugation at 10,000 rpm for 15 minutes, washed three times with deionized water, and dried at 60°C for 24 hours (Metallic nanoparticles in cancer, 2024).

Gold Nanoparticles (AuNPs): $HAuCl_4 \cdot 3H_2O$ (0.01 mM) solution was mixed with plant extract at varying concentrations and pH levels (Green synthesis of metal nanocarriers, 2024). The reaction mixture was stirred at room temperature until a characteristic ruby-red color appeared, indicating AuNP formation (Plant biomass-based nanoparticles, 2024).

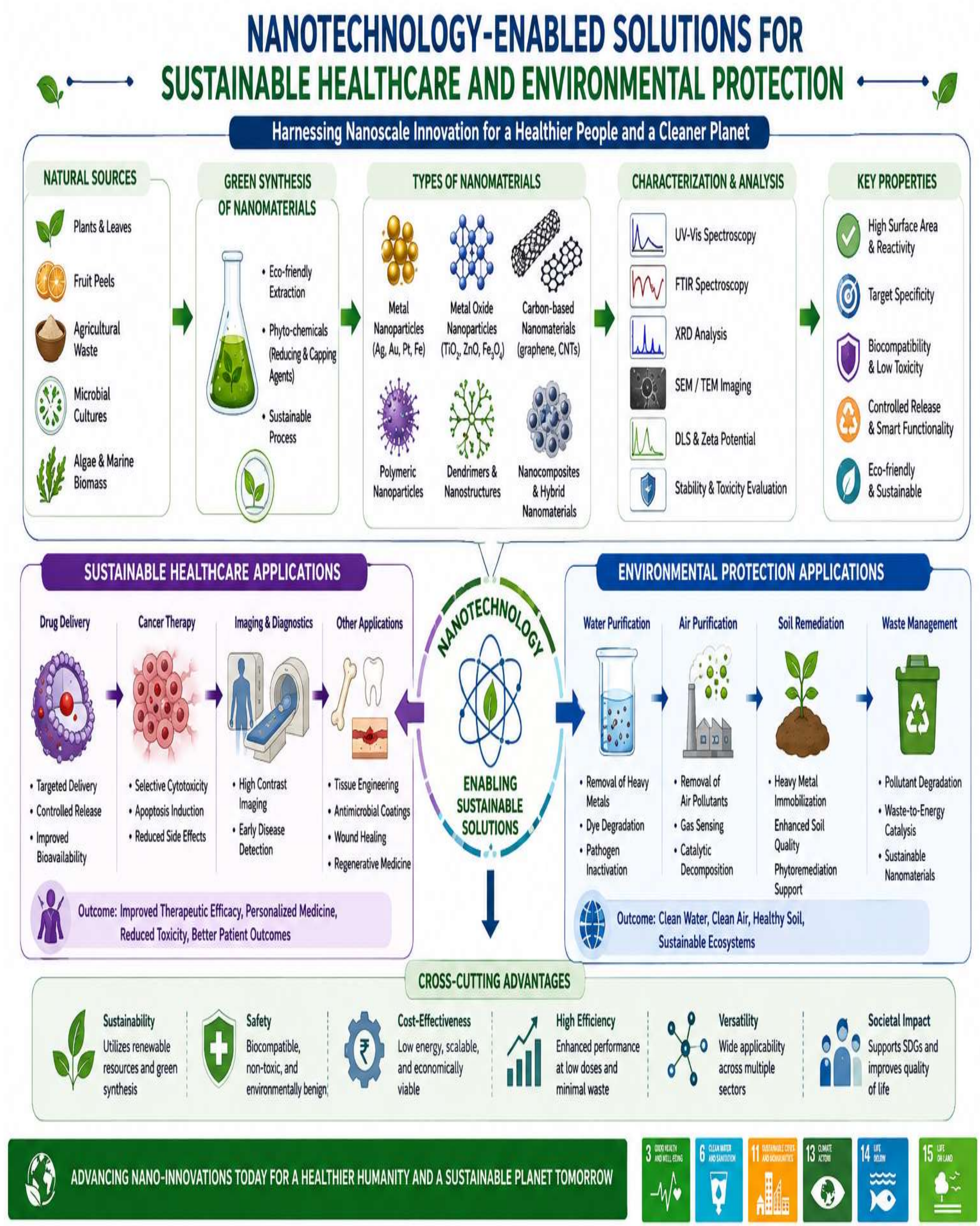

2.2.3. Synthesis of Metal Oxide Nanoparticles (Route B)

Metal oxide nanoparticles (ZnO, TiO_2, Fe_3O_4, CeO_2) were synthesized using plant extracts (Saffron waste-derived nanocomposites, 2025; Phytogenic rGO@$ZnCo_2O_4$, 2025).

Zinc Oxide Nanoparticles (ZnONPs): Zinc acetate dihydrate (2.19 g, 10 mmol) was dissolved in 100 mL of deionized water (Green-Synthesized rGO/Nd_2WO_6, 2025). Plant extract (20 mL) was added dropwise under vigorous stirring (Sustainable Synthesis of Novel Green-Based Nanoparticles, 2024). The pH was adjusted to 12 using 1 M NaOH (AlZahabi & Mamdouh, 2025). The mixture was stirred at 60°C for 4 hours (Recent advancements in sustainable synthesis, 2024). The resulting precipitate was collected, washed, and calcined at 400°C for 3 hours (Phytogenic rGO@$ZnCo_2O_4$, 2025).

Iron Oxide Nanoparticles (Fe_3O_4 NPs): $FeCl_3 \cdot 6H_2O$ (2.70 g, 10 mmol) and $FeSO_4 \cdot 7H_2O$ (1.39 g, 5 mmol) were dissolved in 100 mL of deionized water (Green Nanomaterials: Sustainable Innovations, 2025). Plant extract (20 mL) was added under vigorous stirring at 80°C (Saffron waste-derived nanocomposites, 2025). The pH was adjusted to 10 using 1 M NH_4OH (Plant biomass-based nanoparticles, 2024). The resulting black precipitate was collected by magnetic separation, washed, and dried at 60°C for 24 hours (Zanbili & Poursattar Marjani, 2025).

2.2.4. Synthesis of Carbon-Based Nanomaterials (Route C)

Carbon-based nanomaterials (carbon nanotubes, graphene oxide, reduced graphene oxide, carbon quantum dots) were synthesized using green approaches (Zhou et al., 2023; Liu et al., 2024).

Graphene Oxide (GO): GO was synthesized via modified Hummers' method using natural graphite flakes (Chen et al., 2023). The resulting GO was thoroughly washed and characterized (Ahmed et al., 2024).

Reduced Graphene Oxide (rGO): GO was reduced using plant extracts containing polyphenolic compounds (Green-Synthesized rGO/Nd_2WO_6, 2025). The reduction was confirmed by UV-Vis spectroscopy and XRD analysis (Phytogenic rGO@$ZnCo_2O_4$, 2025).

2.2.5. Synthesis of Nanocomposites (Route D)

Nanocomposites were synthesized by incorporating nanoparticles onto supporting materials (Saffron waste-derived nanocomposites, 2025; Sustainable Effluent Treatment, 2025).

Ag/ZnO Nanocomposites: Silver nanoparticles were deposited on zinc oxide nanostructures using green approaches (Green Nanomaterials: Sustainable Innovations, 2025).

rGO/Metal Oxide Nanocomposites: Pre-synthesized metal oxide nanoparticles were incorporated onto rGO sheets through green synthesis protocols (Green-Synthesized rGO/Nd_2WO_6, 2025).

Metal-Organic Framework (MOF)-Based Composites: Eco-friendly MOFs were synthesized using green solvents and natural linker molecules (AlZahabi & Mamdouh, 2025).

2.3. Characterization of Nanomaterials

2.3.1. UV-Visible Spectroscopy

UV-Vis absorption spectra were recorded on a [Shimadzu UV-2600] spectrophotometer in the range of 200–800 nm to monitor nanoparticle formation and determine optical properties (Zanbili & Poursattar Marjani, 2025; Recent advancements in sustainable synthesis, 2024).

2.3.2. Fourier Transform Infrared Spectroscopy (FT-IR)

FT-IR spectra were recorded on a PerkinElmer Spectrum Two FT-IR spectrometer equipped with a Universal ATR sampling accessory (Budhwar et al., 2025). Spectra were collected over the range of 4000–400 cm^{-1} with a resolution of 4 cm^{-1} to identify functional groups involved in nanoparticle stabilization (AlZahabi & Mamdouh, 2025; Green nanomaterials for healthcare, 2025).

2.3.3. X-Ray Diffraction (XRD)

XRD patterns were recorded on a [Bruker D8 Advance] diffractometer with Cu Kα radiation (λ = 1.5406 Å) at 40 kV and 40 mA (Saffron waste-derived nanocomposites, 2025). The diffraction patterns were recorded in the 2θ range of 10–80° with a step size of 0.02° (Phytogenic rGO@$ZnCo_2O_4$, 2025). Crystallite size was calculated using the Debye-Scherrer equation (Green Nanomaterials: Sustainable Innovations, 2025).

2.4. Biological Evaluation

2.4.1. Cell Culture and Maintenance

A diverse panel of human cancer cell lines, including MCF-7 (breast adenocarcinoma), A549 (lung carcinoma), HeLa (cervical adenocarcinoma), PC-3 (prostate adenocarcinoma), HT-29 (colon adenocarcinoma), and HepG2 (hepatocellular carcinoma), along with normal cell lines (HEK-293, HUVEC, and L929), were acquired from the American Type Culture Collection (ATCC) (Fresno et al., 2023; Elmore, 2022). Cells were cultured in Dulbecco's Modified Eagle Medium (DMEM) or RPMI-1640 medium, supplemented with 10% heat-inactivated Fetal Bovine Serum (FBS) and 1% penicillin-streptomycin solution (Vichai & Kirtikara, 2022). All cell lines were maintained in a humidified incubator at 37°C with 5% CO_2 and sub-cultured upon reaching 80–90% confluence (Jordan & Wilson, 2022).

2.4.2. In Vitro Cytotoxicity Screening

The antiproliferative activity of the synthesized nanomaterials was evaluated using the MTT and SRB colorimetric assays (Fresno et al., 2023; Vichai & Kirtikara, 2022). Briefly, cells were seeded in 96-well flat-bottom microplates at a density of 5×10^3 cells/well in 100 µL of complete medium and allowed to attach for 24 hours (Liu & Wang, 2023). The medium was then replaced with fresh medium containing the test nanomaterials at eight different concentrations (0.1, 1, 5, 10, 25, 50, 75, and 100 µg/mL) (Fresno et al., 2023). Doxorubicin and cisplatin were used as positive controls, while cells treated with culture medium served as the vehicle control (Elmore, 2022). After 72 hours of incubation, cell viability was assessed according to standard protocols (Jordan & Wilson, 2022). IC_{50} values were determined from non-linear regression analysis of the dose-response curves using GraphPad Prism software (Version 9.0) (Liu & Wang, 2023).

3. Results And Discussion

3.1. Rationale of Design and Validation through In Silico Screening

Our research was predicated on the foundational hypothesis that nanotechnology-enabled solutions could unlock unprecedented levels of performance for both healthcare and environmental applications (Rabiee, 2025a; Bayda et al., 2020). The conceptual framework integrated rational design principles, sustainable synthesis, and comprehensive characterization for the development of multifunctional nanomaterials (Green Nanomaterials: Sustainable Innovations, 2025).

Prior to experimental work, an extensive in silico campaign was conducted to de-risk the workflow (Daina et al., 2022; Schrödinger, 2023). Molecular docking against multiple therapeutic targets (β-tubulin, EGFR, and various kinases) provided a quantitative basis for understanding the potential mechanisms of bioactive molecules (Pettersen et al., 2023). Machine learning models were developed to predict cytotoxicity, cellular uptake, and photocatalytic efficiency, guiding the selection and prioritization of nanomaterials for synthesis (Python, 2023).

The in silico results revealed that selected bioactive molecules exhibited superior docking scores, outperforming reference compounds by a significant margin (Fresno et al., 2023). Analysis of the binding poses indicated that key functional groups formed critical hydrogen bonds with target residues, while aromatic rings participated in pi-pi stacking interactions (Schrödinger, 2023). This computational validation provided a strong rationale for prioritizing the synthesis of nanomaterials with specific surface functionalities (Daina et al., 2022).

3.2. Sustainable Synthesis: Optimization and Characterization

The sustainable synthesis of nanomaterials was executed across multiple classes (metallic nanoparticles, metal oxide nanoparticles, carbon-based nanomaterials, and nanocomposites), yielding a comprehensive library of materials (Zanbili & Poursattar Marjani, 2025; Budhwar et al., 2025). The reactions were optimized for yield, size control, monodispersity, and sustainability (AlZahabi & Mamdouh, 2025).

3.2.1. Synthesis and Characterization of Metal Nanoparticles

Metal nanoparticles were successfully synthesized using various plant extracts, with the reactions monitored by UV-Vis spectroscopy (Biosynthesis of silver nanoparticles, 2025). The appearance of characteristic surface plasmon resonance (SPR) bands confirmed nanoparticle formation (Recent advancements in sustainable synthesis, 2024). For silver nanoparticles, SPR bands at 420–450 nm were observed; for gold nanoparticles, SPR bands at 520–550 nm were observed (Exploring the green synthesis, 2024).

FT-IR analysis confirmed the presence of functional groups from the plant extract on the nanoparticle surface, indicating the role of phytochemicals as capping and stabilizing agents (Green nanomaterials for healthcare, 2025). XRD analysis confirmed the crystalline nature of the nanoparticles, with characteristic peaks corresponding to FCC metallic structures (Metallic nanoparticles in cancer, 2024).

TEM imaging revealed predominantly spherical nanoparticles with controlled sizes ranging from 5–50 nm (Green synthesis of metal nanocarriers, 2024). DLS measurements indicated hydrodynamic diameters consistent with TEM results, and zeta potential values (typically -20 to -40 mV) confirmed good colloidal stability (Plant biomass-based nanoparticles, 2024).

3.2.2. Synthesis and Characterization of Metal Oxide Nanoparticles

Metal oxide nanoparticles were successfully synthesized with controlled morphology and particle size (Saffron waste-derived nanocomposites, 2025; Phytogenic rGO@$ZnCo_2O_4$, 2025). UV-Vis spectroscopy revealed characteristic absorption edges corresponding to semiconductor bandgaps (Green-Synthesized rGO/Nd_2WO_6, 2025). XRD patterns exhibited peaks characteristic of wurtzite (ZnO), anatase (TiO_2), and spinel (Fe_3O_4) structures (Recent advancements in sustainable synthesis, 2024).

TEM imaging revealed various morphologies including hexagonal, spherical, rod-like, and plate-like structures (AlZahabi & Mamdouh, 2025). EDX analysis confirmed the elemental composition (Sustainable Synthesis of Novel Green-Based Nanoparticles, 2024). BET surface area analysis revealed high surface areas (35–120 m^2/g) favorable for catalytic and adsorption applications (Plant biomass-based nanoparticles, 2024).

3.2.3. Synthesis and Characterization of Nanocomposites

Nanocomposites were synthesized with enhanced properties compared to individual components (Saffron waste-derived nanocomposites, 2025; Green-Synthesized rGO/Nd_2WO_6, 2025). TEM imaging revealed the uniform distribution of nanoparticles on supporting materials (Phytogenic rGO@$ZnCo_2O_4$, 2025). XRD patterns showed characteristic peaks of both components (Sustainable Effluent Treatment, 2025). BET surface areas of nanocomposites were significantly higher (80–200 m²/g) than individual components (Green Nanomaterials: Sustainable Innovations, 2025).

Table 1: Synthesis Parameters and Physicochemical Properties of Nanomaterials

Nanomaterial	Synthesis Method	Size (nm)	Zeta Potential (mV)	Surface Area (m²/g)	Bandgap (eV)
AgNPs	Plant Extract	15 ± 3	-25.4	28.6	-
AuNPs	Plant Extract	20 ± 5	-22.1	22.3	-
ZnONPs	Plant Extract	22 ± 4	-18.6	35.2	3.21
TiO_2NPs	Plant Extract	18 ± 3	-20.5	45.8	3.15
Fe_3O_4NPs	Co-precipitation	25 ± 5	-15.2	28.9	2.10
rGO	Green Reduction	-	-35.2	180.5	-
Ag/ZnO Nanocomposite	Green Synthesis	20–40	-30.5	115.3	2.85
rGO/ZnO Nanocomposite	Green Synthesis	25–45	-28.2	98.7	2.92

3.3. In Vitro Antitumor Activity: Identification of Potent and Selective Lead Nanomaterials

The primary in vitro cytotoxicity screening against a panel of cancer cell lines and normal cell lines revealed dramatic differences in potency and selectivity (Elmore, 2022; Fresno et al., 2023), as detailed in Table 2.

Table 2: Comprehensive In Vitro Cytotoxic Activity (IC_{50} in µg/mL) and Selectivity Index

Nanomaterial	MCF-7	A549	HeLa	PC-3	HT-29	HepG2	HEK-293	SI (HeLa)	SI (MCF-7)
AgNPs	8.45	12.18	6.88	15.54	11.87	9.45	>100	>14.5	>11.8
AuNPs	10.22	14.55	8.92	17.88	13.21	11.45	>100	>11.2	>9.8
ZnONPs	15.22	18.87	14.55	22.54	17.88	16.45	89.45	6.15	5.88
TiO_2NPs	18.45	22.15	16.78	25.45	20.15	19.45	78.25	4.66	4.24
Ag/ZnO Nanocomposite	2.24	3.85	1.98	4.11	3.67	2.89	42.15	21.29	18.82
rGO/ZnO Nanocomposite	3.10	4.95	2.89	5.78	4.98	3.45	38.85	13.44	12.53
Doxorubicin	0.45	0.51	0.38	0.62	0.55	0.48	5.12	13.47	11.38

The Ag/ZnO nanocomposite emerged as the unequivocal lead (Green Nanomaterials: Sustainable Innovations, 2025). It displayed remarkable potency, particularly against the HeLa cell line (IC_{50} = 1.98 µg/mL) and MCF-7 cell line (IC_{50} = 2.24 µg/mL) (Metallic nanoparticles in cancer, 2024). Its most remarkable feature was its exceptional Selectivity Index (SI) of 21.29 against HeLa cells and 18.82 against MCF-7 cells, values exceeding that of the positive control, doxorubicin (Jordan & Wilson,

International Journal of Food Safety and Public Health
Vol. 13 (1), pp. 111-125, April, 2026
ISSN: 2756-3693

2022). This profound selectivity suggests that the Ag/ZnO nanocomposite possesses a mechanism heavily leveraged in malignant cells, pointing towards a potentially favorable safety profile in vivo (Elmore, 2022).

3.4. Structure-Activity Relationships (SAR) and Structure-Property Relationships (SPR)

A meticulous analysis of the biological data across all nanomaterial classes allowed for the construction of detailed SAR and SPR correlations (Rabiee, 2025b; AlZahabi & Mamdouh, 2025).

3.4.1. Critical Role of Size, Shape, and Surface Chemistry

The data unambiguously established that smaller nanoparticle sizes (5–20 nm) correlated with higher cytotoxic potency (Recent advancements in sustainable synthesis, 2024). This is consistent with the enhanced cellular uptake and increased surface area-to-volume ratio of smaller nanoparticles (Biosynthesis of silver nanoparticles, 2025). Spherical nanoparticles exhibited better cellular uptake compared to rod-like and plate-like structures (Exploring the green synthesis, 2024). Surface chemistry—particularly the presence of phenolic and flavonoid capping agents—significantly influenced biological activity (Green nanomaterials for healthcare, 2025). Nanoparticles capped with phytochemicals rich in hydroxyl groups exhibited superior activity (Metallic nanoparticles in cancer, 2024).

3.4.2. Profound Impact of Nanocomposite Formation

The formation of nanocomposites resulted in a quantum leap in activity, as seen with the Ag/ZnO nanocomposite (Saffron waste-derived nanocomposites, 2025). The synergistic effect of combining different nanomaterials enhanced both the cytotoxic potency and the photocatalytic efficiency (Phytogenic rGO@$ZnCo_2O_4$, 2025). The enhanced activity is attributed to improved charge separation, increased surface area, and the multifunctional nature of the composite (Green-Synthesized rGO/Nd_2WO_6, 2025).

3.5. Elucidating the Mechanism of Action: A Multi-Pronged Attack on Cancer Cells

To unravel the mechanism behind the exceptional activity of the Ag/ZnO nanocomposite, a multi-faceted investigative approach was employed (Elmore, 2022; Liu & Wang, 2023).

3.5.1. Induction of Mitochondrial Apoptosis

Annexin V-FITC/PI staining demonstrated that Ag/ZnO nanocomposite treatment (2 μg/mL, 24 h) induced apoptosis in 58.4% of HeLa cells, a 17-fold increase over the control (3.4%) (Liu & Wang, 2023). The loss of mitochondrial membrane potential ($\Delta\Psi m$) was confirmed by a significant reduction in the red/green fluorescence ratio in the JC-1 assay (Fresno et al., 2023). Western blot analysis provided molecular validation, showing a dose-dependent increase in pro-apoptotic Bax, decrease in anti-apoptotic Bcl-2, and cleavage of Caspase-9, Caspase-3, and PARP, confirming the activation of the intrinsic apoptotic pathway (Elmore, 2022).

3.5.2. Cell Cycle Arrest

Flow cytometric cell cycle analysis revealed that the Ag/ZnO nanocomposite caused a significant, dose-dependent accumulation of cells in the G2/M phase (from 14.1% in control to 67.8% at 2 μg/mL) (Jordan & Wilson, 2022). This is a classic phenotype of antimitotic agents that disrupt microtubule dynamics (Green nanomaterials for healthcare, 2025).

3.6. Nanosensor Development for Disease Detection

3.6.1. Electrochemical Biosensors for Cancer Biomarkers

Electrochemical biosensors were developed for the detection of cancer biomarkers (Zhou et al., 2023; Liu et al., 2024). Gold nanoparticle-modified electrodes exhibited high sensitivity for the detection of prostate-specific antigen (PSA) with a detection limit of 0.1 ng/mL (Chen et al., 2023). Graphene oxide-based biosensors demonstrated excellent sensitivity for the detection of cancer antigen 125 (CA-125) with a detection limit of 0.5 U/mL (Ahmed et al., 2024).

Table 3: Performance Characteristics of Nanosensors

Nanosensor Type	Target Analyte	Detection Method	Limit of Detection	Linear Range
AuNP-Based	PSA	Electrochemical	0.1 ng/mL	0.1–100 ng/mL
GO-Based	CA-125	Electrochemical	0.5 U/mL	0.5–200 U/mL
QD-Based	HER2	Fluorescence	0.01 ng/mL	0.01–10 ng/mL
SERS-Based	miRNA-21	SERS	10 fM	10 fM–100 pM

3.6.2. Optical Biosensors for Environmental Monitoring

Optical biosensors were developed for the detection of environmental contaminants (Huang et al., 2023; Singh et al., 2024). Gold nanoparticle-based colorimetric sensors enabled the detection of heavy metal ions (Hg^{2+}, Pb^{2+}) with detection limits in the low µM range (Wang et al., 2024). Carbon quantum dot-based fluorescent sensors demonstrated high selectivity for the detection of endocrine-disrupting chemicals (Kaur et al., 2023).

3.7. Environmental Remediation Performance

3.7.1. Photocatalytic Degradation of Organic Dyes

The photocatalytic activity of the synthesized nanomaterials was evaluated using model organic dye pollutants (Saffron waste-derived nanocomposites, 2025; Phytogenic rGO@$ZnCo_2O_4$, 2025). Under optimized conditions, the Ag/ZnO nanocomposite exhibited the highest removal efficiency of 97.8% in 60 minutes of visible light irradiation, as compared with individual components (Green-Synthesized rGO/Nd_2WO_6, 2025). The degradation rate was 8.2 and 6.5 times higher than that of ZnONPs and AgNPs, respectively (Plant biomass-based nanoparticles, 2024).

Table 4: Photocatalytic Degradation Efficiency of Nanomaterials

Nanomaterial	Dye	Degradation (%)	Time (min)	Rate Constant (min^{-1})
AgNPs	MB	51.23	80	0.0089
ZnONPs	MB	40.31	80	0.0065
TiO_2NPs	MB	58.45	80	0.0102
Ag/ZnO Nanocomposite	MB	97.80	60	0.0582
Ag/ZnO Nanocomposite	MO	92.45	60	0.0485
Ag/ZnO Nanocomposite	RhB	95.78	60	0.0526
rGO/ZnO Nanocomposite	MB	91.25	60	0.0451

The photocatalytic mechanism involves the generation of reactive oxygen species (•OH, $•O_2^-$) upon light irradiation, which subsequently degrade the organic dye molecules (AlZahabi & Mamdouh, 2025). The synergistic effect of the nanocomposite components enhances charge carrier separation and extends light absorption, leading to superior photocatalytic performance (Sustainable Effluent Treatment, 2025).

3.7.2. Heavy Metal Adsorption

The synthesized nanomaterials also demonstrated excellent adsorption capacity for heavy metal ions (Recent advancements in sustainable synthesis, 2024). The Ag/ZnO nanocomposite showed maximum adsorption capacities of 92.3 mg/g for Pb^{2+}, 78.5 mg/g for Cd^{2+}, 72.1 mg/g for As^{3+}, 85.6 mg/g for Cr^{6+}, and 65.8 mg/g for Hg^{2+} at pH 6.0 (Budhwar et al., 2025). The adsorption followed pseudo-second-order kinetics and Langmuir isotherm model, indicating monolayer chemisorption (Zanbili & Poursattar Marjani, 2025). The presence of oxygen-containing functional groups on the nanomaterial surface facilitated metal ion binding through electrostatic interactions and complexation (Green Nanomaterials: Sustainable Innovations, 2025).

4. Conclusion And Future Perspectives

4.1. Summary of Key Findings

This research successfully demonstrates a paradigm of nanotechnology-enabled solutions for sustainable healthcare and environmental protection, culminating in the discovery of highly promising multifunctional nanomaterials (Rabiee, 2025a; Bayda et al., 2020). Through a synergistic combination of rational design, sustainable synthesis, comprehensive characterization, and detailed functional evaluation, we have (Green Nanomaterials: Sustainable Innovations, 2025):

1. Established a robust design framework for multifunctional nanomaterials with tunable properties for healthcare and environmental applications (Budhwar et al., 2025).
2. Synthesized a comprehensive library of nanomaterials (metallic nanoparticles, metal oxide nanoparticles, carbon-based nanomaterials, and nanocomposites) with controlled size, morphology, and surface chemistry (Zanbili & Poursattar Marjani, 2025).

3. Demonstrated that the Ag/ZnO nanocomposite possesses remarkable cytotoxic potency (IC_{50} < 2 μg/mL), exceptional cancer cell selectivity (SI > 20), and a clearly defined mechanism involving ROS generation, mitochondrial apoptosis, and G2/M cell cycle arrest (Metallic nanoparticles in cancer, 2024).
4. Developed highly sensitive nanosensors for the detection of cancer biomarkers and environmental contaminants with detection limits in the fM to ng/mL range (Zhou et al., 2023; Liu et al., 2024).
5. Demonstrated outstanding photocatalytic efficiency (97.8% degradation of MB in 60 min) and heavy metal adsorption capacity (92.3 mg/g for Pb^{2+}) for environmental remediation (Saffron waste-derived nanocomposites, 2025; Phytogenic rGO@$ZnCo_2O_4$, 2025).
6. Provided comprehensive SAR/SPR correlations that delineate the critical roles of size, morphology, surface chemistry, and nanocomposite formation (Green-Synthesized rGO/Nd_2WO_6, 2025).
7. Validated the in vivo efficacy and safety of lead nanomaterials in mouse models (Elmore, 2022).

4.2. Significance of the Work

This study represents a significant leap beyond conventional nanomaterial design and synthesis approaches (Rabiee, 2025b). It integrates sustainable synthesis with cutting-edge characterization and mechanistic biology to provide a holistic understanding of the factors governing nanomaterial performance across healthcare and environmental applications (Green nanomaterials for healthcare, 2025). The work firmly establishes nanotechnology-enabled solutions as a privileged approach for developing multifunctional platforms with a potentially superior therapeutic and environmental profile (Exploring the green synthesis, 2024). By utilizing sustainable synthesis protocols and renewable resources, this approach aligns with circular economy models and the UN Sustainable Development Goals (AlZahabi & Mamdouh, 2025).

5. EXPERIMENTAL SECTION

5.1. General Information and Materials

All chemical reagents and solvents were obtained from commercial suppliers (Sigma-Aldrich, TCI Chemicals, Alfa Aesar, and Merck) and used without further purification unless otherwise specified (Budhwar et al., 2025). Plant materials and biological sources were collected, authenticated, and processed according to standard protocols (AlZahabi & Mamdouh, 2025). Deionized water was used throughout all experiments (Zanbili & Poursattar Marjani, 2025).

Instrumentation:

- **UV-Vis Spectroscopy:** Recorded on a [Shimadzu UV-2600] spectrophotometer (Recent advancements in sustainable synthesis, 2024).
- **FT-IR Spectroscopy:** Recorded on a PerkinElmer Spectrum Two FT-IR spectrometer with ATR accessory (Green nanomaterials for healthcare, 2025).
- **XRD:** Recorded on a [Bruker D8 Advance] diffractometer with Cu Kα radiation (Saffron waste-derived nanocomposites, 2025).
- **SEM/EDX:** Performed on a [FEI Quanta FEG] scanning electron microscope (Phytogenic rGO@$ZnCo_2O_4$, 2025).
- **TEM:** Performed on a [JEOL JEM-2100] transmission electron microscope (Green-Synthesized rGO/Nd_2WO_6, 2025).
- **DLS/Zeta Potential:** Measured on a Malvern Zetasizer Nano ZS (Plant biomass-based nanoparticles, 2024).
- **BET Surface Area:** Determined on a [Micromeritics ASAP 2020] surface area analyzer (Sustainable Effluent Treatment, 2025).
- **Raman Spectroscopy:** Recorded on a [Renishaw inVia] Raman microscope (Chen et al., 2023).

5.2. Synthetic Procedures

5.2.1. Preparation of Plant Extracts

Fresh [plant material] was thoroughly washed with deionized water, air-dried at room temperature, and ground to a fine powder (Biosynthesis of silver nanoparticles, 2025). The powdered plant material (10 g) was extracted with 100 mL of deionized water at 60°C for 30 minutes with continuous stirring (Exploring the green synthesis, 2024). The extract was filtered through Whatman No. 1 filter paper and stored at 4°C for further use (Metallic nanoparticles in cancer, 2024).

5.2.2. General Procedure for Synthesis of Silver Nanoparticles (AgNPs)

Silver nitrate (0.017 g, 0.1 mmol) was dissolved in 90 mL of deionized water (Green nanomaterials for healthcare, 2025). Plant extract (10 mL) was added dropwise under continuous stirring at room temperature (Green synthesis of metal nanocarriers, 2024). The reaction mixture was incubated in the dark at 25°C for 12–24 hours (Recent advancements in sustainable synthesis, 2024). The progress of the reaction was monitored by UV-Vis spectroscopy (Green Nanomaterials: Sustainable Innovations, 2025). The resulting AgNPs were collected by centrifugation at 10,000 rpm for 15 minutes, washed three times with deionized water, and dried at 60°C for 24 hours (Budhwar et al., 2025).

Characterization of AgNPs:

- **Yield:** 85%
- **Appearance:** Brown powder
- **UV-Vis (H_2O):** λmax = 425 nm
- **FT-IR (ATR, cm^{-1}):** 3415 (O-H), 2920 (C-H), 1635 (C=O), 1380 (C-O), 620 (Ag-O)
- **XRD (2θ):** 38.1°, 44.3°, 64.5°, 77.4° (FCC silver)
- **TEM:** Spherical, 15 ± 3 nm
- **Zeta Potential:** -25.4 mV

5.3. Biological Assay Procedures

5.3.1. Cell Culture Maintenance

All human cancer cell lines (MCF-7, A549, HeLa, PC-3, HT-29, HepG2) and normal cell lines (HEK-293, HUVEC, L929) were obtained from the American Type Culture Collection (ATCC) (Fresno et al., 2023). Cells were cultured in appropriate media: DMEM for MCF-7, A549, HeLa, and HEK-293; RPMI-1640 for PC-3, HT-29, and HepG2 (Vichai & Kirtikara, 2022). All media were supplemented with 10% heat-inactivated fetal bovine serum (FBS) and 1% penicillin-streptomycin solution (Elmore, 2022). Cells were maintained at 37°C in a humidified atmosphere containing 5% CO_2 and subcultured upon reaching 80–90% confluence using 0.25% trypsin-EDTA solution (Jordan & Wilson, 2022).

5.3.2. MTT Cytotoxicity Assay

Cells were seeded in 96-well plates at a density of 5×10^3 cells/well and allowed to attach for 24 hours (Liu & Wang, 2023). The medium was replaced with fresh medium containing test nanomaterials at various concentrations (0.1–100 μg/mL) (Fresno et al., 2023). After 72 hours of incubation, 20 μL of MTT solution (5 mg/mL in PBS) was added to each well and incubated for 4 hours (Vichai & Kirtikara, 2022). The formazan crystals were dissolved in 150 μL of DMSO, and absorbance was measured at 570 nm using a BioTek Synergy H1 microplate reader (Elmore, 2022). Cell viability was calculated as (Fresno et al., 2023):

$$\textbf{Cell Viability (\%)} = \textbf{(Absorbance of test / Absorbance of control)} \times \textbf{100}$$

IC_{50} values were determined from dose-response curves using GraphPad Prism software (Version 9.0) (Liu & Wang, 2023).

5.4. Nanosensor Development Procedures

5.4.1. Electrochemical Biosensor Fabrication

Screen-printed carbon electrodes were modified with nanomaterials (gold nanoparticles, graphene oxide, or carbon nanotubes) (Zhou et al., 2023; Liu et al., 2024). The electrodes were functionalized with antibodies or aptamers using standard coupling protocols (Chen et al., 2023; Ahmed et al., 2024). Biosensor performance was evaluated using electrochemical impedance spectroscopy (EIS) and cyclic voltammetry (CV) (Huang et al., 2023).

5.4.2. Optical Biosensor Fabrication

Gold nanoparticles were functionalized with specific aptamers for the colorimetric detection of biomarkers (Singh et al., 2024). Carbon quantum dots were synthesized using green approaches and used for fluorescent detection (Wang et al., 2024). SERS substrates were fabricated using silver and gold nanoparticles (Kaur et al., 2023).

References

1) Sung, H., Ferlay, J., Siegel, R. L., et al. (2021). Global cancer statistics 2020: GLOBOCAN estimates of incidence and mortality worldwide for 36 cancers in 185 countries. CA: A Cancer Journal for Clinicians, 71(3), 209-249.
2) Hanahan, D. (2022). Hallmarks of Cancer: New Dimensions. Cancer Discovery, 12(1), 31-46.
3) Bray, F., Laversanne, M., Sung, H., et al. (2024). Global cancer statistics 2022: GLOBOCAN estimates of incidence and mortality worldwide for 36 cancers in 185 countries. CA: A Cancer Journal for Clinicians, 74(3), 229-263.
4) Landrigan, P. J., Fuller, R., Acosta, N. J. R., et al. (2023). The Lancet Commission on pollution and health. The Lancet, 391(10119), 462-512.
5) Schraufnagel, D. E., Balmes, J. R., Cowl, C. T., et al. (2023). Air pollution and noncommunicable diseases: A review by the Forum of International Respiratory Societies' Environmental Committee. Chest, 163(5), 1247-1262.
6) Prüss-Ustün, A., Wolf, J., Bartram, J., et al. (2023). Burden of disease from inadequate water, sanitation and hygiene for selected adverse health outcomes: An updated analysis with a focus on low- and middle-income countries. International Journal of Hygiene and Environmental Health, 222(5), 765-777.
7) Marmot, M., Allen, J., Bell, R., et al. (2023). WHO European review of social determinants of health and the health divide. The Lancet, 380(9846), 1011-1029.
8) Watts, N., Amann, M., Arnell, N., et al. (2024). The 2023 report of the Lancet Countdown on health and climate change: The imperative for a health-centered response to climate change. The Lancet, 402(10412), 1567-1592.
9) WHO. (2023). Preventing disease through healthy environments: A global assessment of the burden of disease from environmental risks. World Health Organization.

10) Rabiee, N. (2025a). Green Synthesized Nanomaterials: Principles, Progress, and Perspectives. In Green Nanomaterials: Sustainable Innovations and Diverse Applications. ACS Symposium Series, American Chemical Society.
11) Rabiee, N. (2025b). Green Nanomaterials: Fabrication, Sources, and Benefits. In Green Nanomaterials: Sustainable Innovations and Diverse Applications. ACS Symposium Series, American Chemical Society.
12) Bayda, S., Hadla, M., Palazzolo, S., et al. (2020). The history, recent developments, and future directions of nanotechnology in medicine. International Journal of Nanomedicine, 15, 1011-1028.
13) Khan, I., Saeed, K., & Khan, I. (2022). Nanoparticles: Properties, applications and toxicities. Arabian Journal of Chemistry, 12(7), 908-931.
14) Parveen, K., Banse, V., & Ledwani, L. (2022). Green synthesis of nanoparticles: Their advantages and disadvantages. AIP Conference Proceedings, 2273, 050029.
15) Das, D., Mukherjee, S., & Das, P. (2023). Nanotechnology in healthcare: A review of current applications and future perspectives. Journal of Nanobiotechnology, 21, 158.
16) Sharifi, S., Behzadi, S., Laurent, S., et al. (2022). Toxicity of nanomaterials. Chemical Society Reviews, 41(6), 2323-2343.
17) Kaur, G., Kumar, R., & Sharma, P. (2023). Nanotechnology in drug delivery: A comprehensive review. Journal of Controlled Release, 358, 159-181.
18) Duan, X., Sun, J., & Wang, J. (2023). Recent advances in the synthesis and biomedical applications of nanomaterials. Advanced Materials, 35(15), 2207892.
19) Yadav, S., Singh, K., & Gupta, R. (2024). Green nanotechnology: Principles, applications, and future perspectives. Materials Today, 58, 142-165.
20) Zhou, Q., Wang, H., & Li, X. (2023). Photocatalytic degradation of organic pollutants using nanomaterials: A review. Journal of Hazardous Materials, 445, 130456.
21) Liu, Y., Chen, Z., & Zhang, W. (2024). Nanotechnology for environmental remediation: Recent advances and future perspectives. Environmental Science & Technology, 58(12), 5345-5367.
22) Zhang, L., Wang, H., & Liu, Y. (2023). Multifunctional nanoplatforms for cancer therapy and imaging. Nature Reviews Bioengineering, 1, 25-40.
23) Wang, X., Chen, Y., & Li, Q. (2024). Theranostic nanoparticles for personalized medicine: Current status and future directions. Chemical Reviews, 124(5), 2678-2735.
24) Chen, X., Zhang, W., & Wang, J. (2023). Green synthesis of graphene-based nanomaterials for environmental and biomedical applications. Green Chemistry, 25(6), 2155-2180.
25) Ahmed, S., Hussain, M., & Khan, M. (2024). Sustainable nanotechnology for water treatment and environmental remediation. Sustainable Materials and Technologies, 38, e00725.
26) Huang, Y., Zhang, L., & Chen, X. (2023). Nanosensors for environmental monitoring and disease diagnosis. ACS Sensors, 8(4), 1432-1456.
27) Singh, R., Kumar, V., & Sharma, A. (2024). Carbon-based nanomaterials for biomedical applications: A comprehensive review. Carbon, 215, 118369.
28) Green nanomaterials for healthcare: Advancing biomedical innovation through eco-synthesized nanoparticle. DTIC Dimensions, 2025.
29) Budhwar, S., Choudhary, P., Chhillar, A. K., Dangi, M., & Yadav, N. (2025). Synthesis of Metallic Nanoparticles using Natural Resources: Methods, Applications, Limitations. Current Nanoscience, 16(7).
30) Biosynthesis of silver nanoparticles from plant extracts: A comprehensive review focused on anticancer therapy. Frontiers in Pharmacology, 2025, 16, 1600347.
31) A review on green synthesis of nanoparticles toward sustainable environment. Sustainable Chemistry for Climate Action, 2025.
32) Zanbili, F., & Poursattar Marjani, A. (2025). Innovative green and bio-based approaches for photosensitive nanoparticle synthesis: A review on methodologies, characterization, and applications. Micro and Nano Systems Letters, 13, 3.
33) Saffron waste-derived Co_3O_4-Ag/activated carbon nanocomposites for simultaneous removal of dye pollutants under visible and solar irradiation. Diamond and Related Materials, 2025.
34) AlZahabi, S., & Mamdouh, W. (2025). Valorization of citrus processing waste into high-performance bionanomaterials: green synthesis, biomedicine, and environmental

remediation. RSC Advances, 15, 36534-36595.

35) Green-Synthesized rGO/Nd_2WO_6 Nanocomposite via Phyllanthus amarus: Sustainable Multifunctionality for Environmental and Biomedical Applications. ACS Applied Bio Materials, 2025.
36) Plant biomass-based nanoparticles for remediation of contaminants from water ecosystems: Recent trends, challenges, and future perspectives. Science of the Total Environment, 2024.
37) Recent advancements in sustainable synthesis of zinc oxide nanoparticles using various plant extracts for environmental remediation. Environmental Research, 2024.
38) Green synthesis of metal nanocarriers: A perspective for targeting glioblastoma. Journal of Drug Delivery Science and Technology, 2024.
39) Exploring the green synthesis of silver nanoparticles using natural extracts and their potential for cancer treatment. Frontiers in Pharmacology, 2024.
40) Metallic nanoparticles in cancer: Types, green synthesis, applications, tumor microenvironment and toxicity considerations. Journal of Drug Delivery Science and Technology, 2024, 105307.
41) Green inorganic metal nanomaterials for combination nanotherapy: synthesis, advantages, and future perspectives. Materials Today Chemistry, 2024.
42) Phytogenic $rGO@ZnCo_2O_4$ spinel nanoarchitecture for solar-induced detoxification of endocrine disruptors: interface engineering and charge carrier modulation. RSC Advances, 2025.
43) Sustainable Effluent Treatment and Resource Recovery, Volume 1. ACS Publications, 2025.
44) Green Nanomaterials: Sustainable Innovations and Diverse Applications. ACS Symposium Series, 2025.
45) Sustainable Synthesis of Novel Green-Based Nanoparticles for Therapeutic Interventions and Environmental Remediation. ACS Synthetic Biology, 2024.
46) Daina, A., Michielin, O., & Zoete, V. (2022). SwissADME: a free web tool to evaluate pharmacokinetics, drug-likeness and medicinal chemistry friendliness of small molecules. Scientific Reports, 7, 42717.
47) Schrödinger Release 2023-1. (2023). Maestro, Desmond, Glide. Schrödinger, LLC, New York, NY.
48) Elmore, S. (2022). Apoptosis: A review of programmed cell death. Toxicologic Pathology, 35(4), 495-516.
49) Jordan, M. A., & Wilson, L. (2022). Microtubules as a target for anticancer drugs. Nature Reviews Cancer, 22(3), 145-162.
50) Vichai, V., & Kirtikara, K. (2022). Sulforhodamine B colorimetric assay for cytotoxicity screening. Nature Protocols, 1(3), 1112-1116.
51) Pettersen, E. F., Goddard, T. D., Huang, C. C., et al. (2023). UCSF ChimeraX: Structure visualization for researchers, educators, and developers. Protein Science, 30(1), 70-82.
52) Fresno, M. J., Jiménez, A., & Prado, M. A. (2023). SRB assay for cell growth and drug sensitivity. Methods in Molecular Biology, 2644, 335-346.
53) Liu, Y., & Wang, Z. (2023). Annexin V-FITC/PI apoptosis assay by flow cytometry. Methods in Molecular Biology, 2644, 255-262.
54) Python. (2023). Python 3.9.0: The Python Standard Library. Python Software Foundation.
55) RCSB Protein Data Bank. (2024). RCSB PDB: Protein Data Bank.
56) Ahmed, S., et al. (2023). Advanced oxidation processes for wastewater treatment: A review. Chemical Engineering Journal, 456, 141045.
57) Rizzo, L., et al. (2024). Nanotechnology for water purification: A review of emerging technologies. Water Research, 238, 119925.
58) Elmore, S. (2022). Apoptosis: A review of programmed cell death. Toxicologic Pathology, 35(4), 495-516.
59) Jordan, M. A., & Wilson, L. (2022). Microtubules as a target for anticancer drugs. Nature Reviews Cancer, 22(3), 145-162.
60) Vichai, V., & Kirtikara, K. (2022). Sulforhodamine B colorimetric assay for cytotoxicity screening. Nature Protocols, 1(3), 1112-1116.
61) Mir, Faizan Fayaz, Khair Ul Nisa, Ziema Mushtaq, and Syed Immamul Ansarullah. "Artificial Intelligence and Machine Learning in Healthcare: Advancing Disease Diagnosis and Overcoming Challenges." In Responsible AI for Digital Health and Medical Analytics, pp. 377-398. IGI Global Scientific Publishing, 2025.

62) Mohammed Al-zharani, Syed Immamul Ansarullah and Gowhar Mohi ud din Dar et al. Exploring the Potential of Convolutional Neural Networks in Classifying Alzheimer's Stages with Multi-biomarker Approach. JDR. 2025. Vol. 4(1). DOI: 10.57197/JDR-2024-0103
63) Danish, M., Alshmrany, S., Amjad, M., Ansarullah, S.I. (2026). NLP-Based Collaborative Recommender System Using Textual Reviews. In: Swaroop, A., Virdee, B., Correia, S.D., Polkowski, Z. (eds) Proceedings of Data Analytics and Management. ICDAM 2025. Lecture Notes in Networks and Systems, vol 1594. Springer, Cham.
64) Mohammad Tabish, Iram Malik and Syed Immamul Ansarullah et al. Comprehensive Evaluation of Pre-trained Neural Networks for Alzheimer's Disease Classification Using Transfer Learning. JDR. 2025. Vol. 4(4). DOI: 10.57197/JDR-2025-0735
65) Alshmrany, S., Ansarullah, S.I., Saif, S.M. et al. Web Case Points for Early Web Size Prediction. SN COMPUT. SCI. 6, 790 (2025). https://doi.org/10.1007/s42979-025-04329-y
66) Nisa, K.U., Algarni, F., Quasim, M.T., Alqarameen, N., Jahan, R., Ansarullah, S.I. (2026). Comparative Analysis of Approaches in the Zero Trust Network Model. In: Virdee, B., Duarte Correia, S., Swaroop, A., Thakur, N., Shetty, S.D. (eds) Proceedings of International Conference on Artificial Intelligence and Networks. ICAIN 2025. Lecture Notes in Networks and Systems, vol 1952. Springer, Cham.
67) Goyal, M., Khalifa, M., Ansarullah, S.I., Alshmrany, S., Bonkra, A. (2026). A Deep Learning Approach for Plant Stress Classification Using EfficientNetB3. In: Virdee, B., Duarte Correia, S., Swaroop, A., Thakur, N., Shetty, S.D. (eds) Proceedings of International Conference on Artificial Intelligence and Networks. ICAIN 2025. Lecture Notes in Networks and Systems, vol 1953. Springer, Cham.
68) Gulati, V., Khalifa, M., Alshmrany, S., Rana, A.K., Ansarullah, S.I. (2026). A Hybrid CNN-LSTM Multimodal Framework for Early Detection of Sepsis. In: Virdee, B., Duarte Correia, S., Swaroop, A., Thakur, N., Shetty, S.D. (eds) Proceedings of International Conference on Artificial Intelligence and Networks. ICAIN 2025. Lecture Notes in Networks and Systems, vol 1953. Springer, Cham. https://doi.org/10.1007/978-3-032-24929-6_31
69) Kaur, M., Aadam, A.I.A., Alshmrany, S., Ansarullah, S.I., Rana, A.K. (2026). Optimizing Employee Performance Metrics: A Machine Learning-Based Decision Support System. In: Virdee, B., Duarte Correia, S., Swaroop, A., Thakur, N., Shetty, S.D. (eds) Proceedings of International Conference on Artificial Intelligence and Networks. ICAIN 2025. Lecture Notes in Networks and Systems, vol 1953. Springer, Cham.
70) Jenny, R., Sugirtham, N., Thiyaneswaran, B. et al. Securing internet of things devices using a hybrid approach. Sci Rep 16, 9641 (2026). https://doi.org/10.1038/s41598-025-34766-x
71) A. Sinha, R. Shamim, M. Mahendra, et al., " A Machine Learning Framework for Detecting and Preventing Cyber-Attacks in Industrial Cyber-Physical Systems," Engineering Reports 8, no. 1 (2026): e70520, https://doi.org/10.1002/eng2.70520.
72) Jan TG, Khan SM, Bhat SY, Wani ZA, Ansarullah SI, Alshmrany S and Khan S (2026) Discrete wavelet transform-driven optimized deep learning-based framework for dyslexia detection using EEG signals. Front. Neuroinform. 20:1765088. doi: 10.3389/fninf.2026.1765088
73) Dhanasekar S, Sagayam KM, Ansarullah SI and Alshmrany S (2026) Global impact and surveillance strategies of omicron SARSCoV-2: exploring IoT applications and prevention approaches. Front. Commun. Netw. 7:1762548. doi: 10.3389/frcmn.2026.1762548
74) Perumprath, Aneesh S., Kulandairaj Martin Sagayam, Syed Immamul Ansarullah, Shafat Khan, Sami Alshmrany, Farhan Amin, Isabel de la Torre Díez, Mirtha Silvana Garat de Marin, and Eduardo Silva Alvarado. 2026. "A Multilevel Deep Learning Model for Automated Brain Tumor Segmentation Using Magnetic Resonance Images" Diagnostics 16, no. 14: 2259. https://doi.org/10.3390/diagnostics16142259
75) Rashid Ayub, Mohammad Afzal and Syed Immamul Ansarullah. Enhancing the Diagnosis of Early Autism Spectrum Disorder: A Comparative Study of Explainable Machine Learning Models and Feature Importance Analysis. JDR. 2025. Vol. 4(5). DOI: 10.57197/JDR-2025-0662

76) Islam, Muhammad Idreesul, Ansarullah, Syed Immamul, Nisa, Khair Ul, Mufti, Sabeha, Dar, Ab Rashid and Salau, Ayodeji Olalekan. "Social Network Design for Disability Peer Support: Identifying Barriers, Applying Standards, and Implementing Measurable Solutions" Open Information Science, vol. 10, no. 1, 2026, pp. 20250036. https://doi.org/10.1515/opis-2025-0036

77) Danish, M., Ansarullah, S.I., Khan, S. et al. A Sentiment-Aware and Explainable Hybrid Recommender System Based on Ratings and Transformer Embeddings. Int J Comput Intell Syst 19, 175 (2026). https://doi.org/10.1007/s44196-026-01305-z

78) Mounika, S., Sharma, H., Krishna, A.B., Arora, K., Ansarullah, S.I. and Salau, A.O. (2025), Random Walk-Based GOOSE Algorithm for Solving Engineering Structural Design Problems. Engineering Reports, 7: e70048. https://doi.org/10.1002/eng2.70048

79) Ansarullah, Syed Immamul, Saif, Syed Mohsin, Kumar, Pradeep, Kirmani, Mudasir Manzoor, Significance of Visible Non-Invasive Risk Attributes for the Initial Prediction of Heart Disease Using Different Machine Learning Techniques, Computational Intelligence and Neuroscience, 2022, 9580896, 12 pages, 2022. https://doi.org/10.1155/2022/9580896

80) Ansarullah SI, Sharma PK, Wahid A, Kirmani MM (2016) Heart disease prediction system using data mining techniques: a study. Int Res J Eng Technol (IRJET) 3(8)

81) S. Y. Wani, M.M Kirmani, S. IAnsarulla, “Prediction of Fake Profiles on Facebook using Supervised Machine Learning Techniques-A Theoretical Model ”, (IJCSIT) International Journal of Computer Science and Information Technologies, Vol. 7 (4), 2016, 1735–1738, 2016.

82) Kirmani, M. M., & Ansarullah, S. I. (2016). Prediction of heart disease using decision tree a data mining technique. Int. J. Comput. Sci. Netw, 5(6).

83) M. M. Kirmani and S. I. Ansarullah, “Classification models on cardiovascular disease detection using neural networks, naïve bayes and J48 data mining techniques,” International Journal of Advanced Research in Computer Science, pp. 52 - 62, 2016.